International Journal of Applied Mechanics
Vol. 8, No. 7 (2016) 1640001 (12 pages)

DOI: 10.1142/S1758825116400019

Rupture of Polydomain and Monodomain Liquid Crystal Elastomer

Wei Fan, Zhijian Wang and Shengqiang Cai*
Department of Mechanical and Aerospace Engineering
University of California, San Diego
La Jolla, CA 92093, USA
**shqcai@ucsd.edu*

Received 17 September 2016
Revised 25 October 2016
Accepted 28 October 2016
Published 16 December 2016

Liquid crystal elastomer (LCE) has been recently explored extensively to make diverse active structures and devices. Depending on synthetic process, LCE can be made either polydomain or monodomain when ambient temperature is below isotropic clearing temperature. In the applications, LCE may be subjected to large mechanical stretch or force and break apart. The capability of predicting the rupture of LCE under different loading conditions is crucial for the applications. However, according to our knowledge, there is no report on fracture energy measurement of LCE. In this paper, we measured fracture energy of both monodomain and polydomain LCEs using pure shear test. We found that polydomain LCE has significantly higher fracture energy than monodomain one. We suggest that the increase of fracture energy in polydomain LCE is attributed to stretch-induced polydomain-to-monodomain transition near the crack tip of the material.

Keywords: Liquid crystal elastomer; fracture energy; pure shear test.

1. Introduction

A combination of liquid crystal and polymeric network can form a new material — liquid crystal elastomers (LCEs). The special molecular combination endows LCEs with many unique properties such as soft elasticity [Dey *et al.*, 2013; Biggins *et al.*, 2012; Brown and Adams, 2012; Adams and Warner, 2005] and multi-responsiveness [Corbett and Warner, 2009; Dawson *et al.*, 2011; Finkelmann and Shahinpoor, 2002; Petsch *et al.*, 2014; Xing *et al.*, 2015], which have led to myriad applications ranging from artificial muscle [Finkelmann and Shahinpoor, 2002; Li and Keller, 2006] to stretchable optical devices [Schmidtke *et al.*, 2005; Shilov *et al.*, 1998; Schmidtke *et al.*, 2002; Dawson *et al.*, 2011]. Recently, several biological materials such as actin

*Corresponding author.

filament network [Dalhaimer *et al.*, 2007] and fibrillar collagens [Knight and Vollrath, 2002] have also been found to have similar molecular structure and behaviors as synthesized LCEs.

Depending on the ambient temperature, liquid crystal molecules, also called mesogens, in LCEs can be either in crystal state when temperature is lower than isotropic clearing temperature or amorphous state when temperature is higher than isotropic clearing temperature. Without special treatment during the synthesis, LCEs are usually fabricated in polydomain state with very fine texture of mesogenic orientations. Mesogens align well inside one domain, but the alignment varies from one domain to another, which makes the polydomain LCE opaque. A mechanical stretch can make polydomain LCE transit to monodomain state which is highly transparent. Release of the stretch will make LCE turn back to polydomain [Clarke *et al.*, 1997].

To directly synthesize monodomain LCE, Küpfer and Finkelmann [1991] firstly introduced two-step crosslinking synthesis. In the experiments, two crosslinking reactions with very different reaction rates were used in synthesizing LCEs. After the completion of the fast crosslinking reaction, uniaxial stress was applied onto a loosely (1st)-crosslinked LCE. The slow crosslinking reaction then proceeded inside the stretched LCE. Finally, a monodomain LCE was obtained and all mesogens oriented toward the stretch direction. Currently, it is still the most commonly adopted method to fabricate monodomain LCE.

Since LCE was synthesized, mechanical properties of it have been intensively studied. For instance, soft elasticity in LCEs associated with stretch-induced rotation of mesogens has been modeled and experimentally demonstrated [Warner, 1999; Warner and Terentjev, 2003; Stenull and Lubensky, 2005]. Unusual temperature-dependent viscoelastic behaviors of LCEs have been recently uncovered experimentally [Azoug *et al.*, 2016]. The interplay of thermal field, electrical field, optical field and mechanics in LCEs has also been studied by different researchers [Camacho-Lopez *et al.*, 2004; Dawson *et al.*, 2011; Lehmann *et al.*, 2001; Thomsen *et al.*, 2001].

For many applications of LCE, they may be subjected to large mechanical stretch or force. When the stretch or force is too large, LCE may break. Therefore, it is of great importance to be able to predict the rupture of LCE under different loading conditions. Although mechanical behaviors of LCE have been intensively studied as discussed above, according to our knowledge, no results have been reported on the rupture of LCEs. In this paper, we experimentally studied the rupture of both polydomain and monodomain LCEs. From the measurements, we found out fracture energy of polydomain LCE is significantly higher than that of monodomain LCE.

2. Materials and Methods

In the experiment, we synthesized both polydomain and monodomain LCEs by following a recently developed method [Yakacki *et al.*, 2015].

2.1. *Chemicals*

1,4-bis-[4-(3-acryloyloxypropyloxy) benzoyloxy]-2-methylbenzene (RM257, Wilshire company, 95%), (2-hydroxyethoxy)-2-methylpropiophenone (HHMP, Sigma-Aldrich, 98%), 2,2′-(ethylenedioxy) diethanethiol (EDDET, Sigma-Aldrich, 95%), pentaerythritol tetrakis (3-mercaptopropionate) (PETMP, Sigma-Aldrich, 95%) and dipropylamine (DPA, Sigma-Aldrich, 98%) were used as received without further purification.

2.2. *LCE synthesis*

12.00 g RM257, the diacrylate mesogen, was dissolved in toluene and the mixture was heated at 85°C to be homogenous. Then, 0.0772 g HHMP as the crosslinking initiator in the second polymerization stage was added into the solution and heated to be dissolved. After that, 2.7360 g EDDET which acts as the flexible spacer in the LCE, and 0.6996 g PETMP, the tetra-arm thiol crosslinker, were added into the stirring RM257 solution dropwise. The Michael addition reaction catalyst 0.0378 g DPA was added later. The mixture was degassed in the vacuum to remove the bubbles inside and poured into a rectangular glass mold with the thickness of 0.5 mm for polydomain LCE samples and 1 mm for monodomain LCE samples. The reaction proceeded at the room temperature overnight. In this step, the thiol groups will react with the acrylate groups in RM257 via Michael addition reaction to form the first crosslinking network.

After putting into the oven for 24 h to evaporate the toluene, the film was uniaxially stretched and placed under 365 nm UV light (UVP High-Intensity UV Inspection Lamp, 100 W) for 15 min to complete the second crosslinking reaction. The stretch ratio λ_{pre} varies from 1 to 5 (1 means no stretch). Figure 1 sketches the synthesis procedure. Depending on the magnitude of λ_{pre}, LCE films with different alignment of mesogens can be obtained. When $\lambda_{\text{pre}} = 1$, polydomain LCE film can be obtained. When $\lambda_{\text{pre}} = 5$, monodomain LCE film with the best alignment can be obtained.

2.3. *Measurement of fracture energy of LCEs*

We adopted pure shear test, first introduced by Rivlin and Thomas [1953], to measure fracture energy of LCEs. The way of calculating fracture energy of LCEs is sketched in Fig. 2. For the LCE samples synthesized in the same condition, three identical experiments were conducted. As shown in the inset of Fig. 2, we denote the length, height and thickness of a LCE sample in the undeformed state by L, H and B. We denote the height of the LCE sample after stretch by h. In our experiments, the length L was 10 times of the height H, and for precut samples, a crack with length $C = 4H$ was introduced in the length direction by a razor blade as shown in Fig. 2. A LCE thin film was glued onto thin acrylic plates, and then the acrylic plates were clamped by the grippers of mechanical testing machine (Instron 5965)

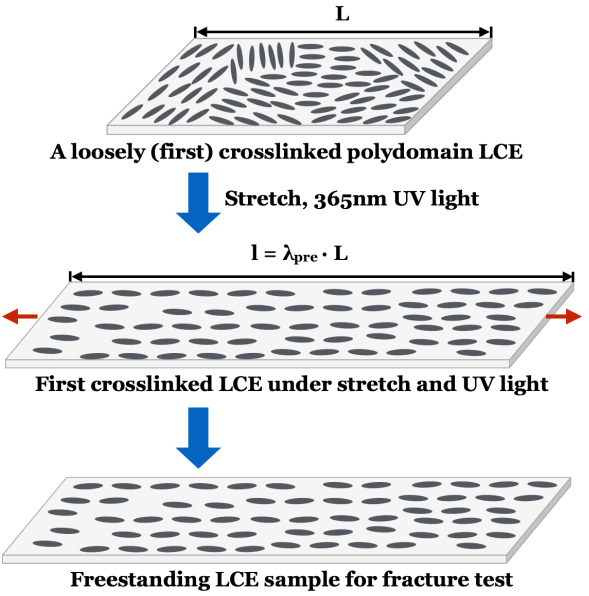

Fig. 1. Schematics of LCE fabrication. During the synthesis, a loosely crosslinked polydomain LCE is stretched uniaxially with stretch ratio λ_{pre} varying from 1 to 5 and subjected to the illumination of UV light for 15 min. During the illumination of UV light, second crosslink forms in the LCE. Monodomain LCE can be maintained in freestanding state for the subsequent fracture test. The elliptical rods in the schematics represent liquid crystal molecules.

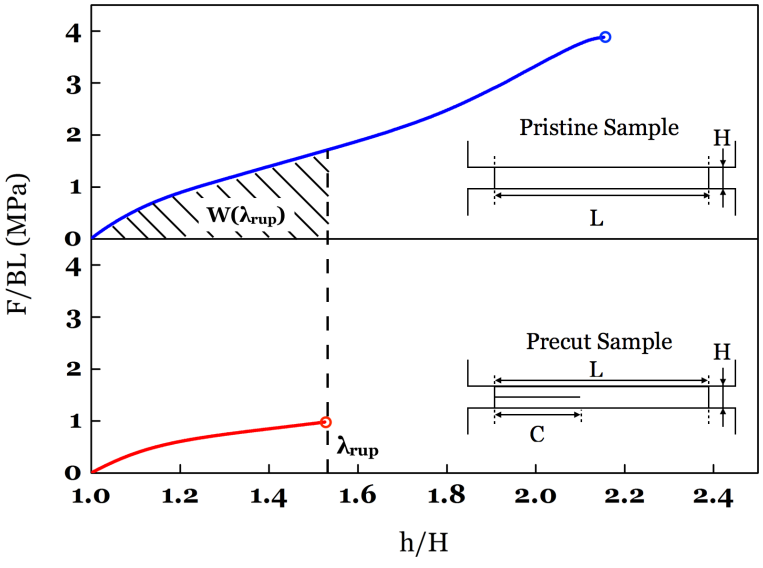

Fig. 2. Schematics of the way to measure fracture energy of a LCE through pure shear test. We first measure stress-stretch curve of a pristine LCE sample as shown on the top panel, and then measure the stress-stretch curve of the same sample with a precut as shown on the bottom. Fracture energy of the LCE can be calculated as $\Gamma = W(\lambda_{\text{rup}}) \cdot H$, where $W(\lambda_{\text{rup}})$ is the area of the shade zone. The circles at the end of the two curves represent the rupturing points.

with a 1000 N load cell. Stretch was along the height direction with the stretch rate of 0.3/min. During the test, no detectable temperature change has been observed in the sample.

As shown in Fig. 2, fracture energy Γ was computed as the equation below, which was firstly given by Rivlin and Thomas [1953],

$$\Gamma = W(\lambda_{\text{rup}}) \cdot H, \tag{1}$$

λ_{rup} is stretch at rupture for the LCE sample with a precut, $W(\lambda_{\text{rup}})$ is strain energy density of pristine LCE sample with stretch λ_{rup}. The above formula can be understood as follows: in the pure shear test sketched in Fig. 2, as the crack grows by the length A, the elastic energy stored in the elastomeric thin film with the width A is released. Consequently, fracture energy of the elastomer can be computed by Eq. (1). Because $W(\lambda_{\text{rup}})$ in Eq. (1) is directly measured experimentally, the equation is valid regardless of the specific form of the constitutive model of the elastomer.

3. Results and Discussion

3.1. *Pure shear test of pristine polydomain and monodomain LCEs*

Figure 3(a) shows the stress-stretch curves of pristine polydomain LCEs under pure shear test. When the stretch is beyond a certain value, softening can be clearly detected from the stress-stretch curves, which usually refers to semi-soft elasticity as described in the literature [Warner, 1999]. In the experiment, opaque polydomain LCEs become transparent when the stretch is large. It has been known [Küpfer and Finkelmann, 1991; Clarke *et al.*, 1997] that such material softening and optical transparency transition are correlated to polydomain-to-monodomain transition in the LCEs induced by mechanical stretch.

Figures 3(b) and 3(c) plot measured stress-stretch curves of pristine monodomain LCEs with four different applied prestretches during their second crosslinking stage. In Fig. 3(b), the tensile direction is perpendicular to the prestretch direction, while the tensile direction is parallel to the prestretch direction in Fig. 3(c). It can be seen clearly from Figs. 3(b) and 3(c), mechanical properties of LCEs strongly depend on the magnitude of applied prestretch during their second crosslinking stage and are also highly anisotropic. Similar to Fig. 3(a), when the tensile direction is perpendicular to the prestretch direction, rotation of mesogenic molecules toward the tensile direction results in material softening as shown in Fig. 3(b). Mechanical stiffness is much higher in monodomain LCEs in the direction parallel to the prestretch direction as shown in Fig. 3(c). The larger prestretch applied to the LCEs during the second crosslinking stage, the higher stiffness of the LCEs along the prestretch direction. When the tensile direction is parallel to the prestretch direction, rotation of mesogenic molecules contributes negligibly to the overall strain.

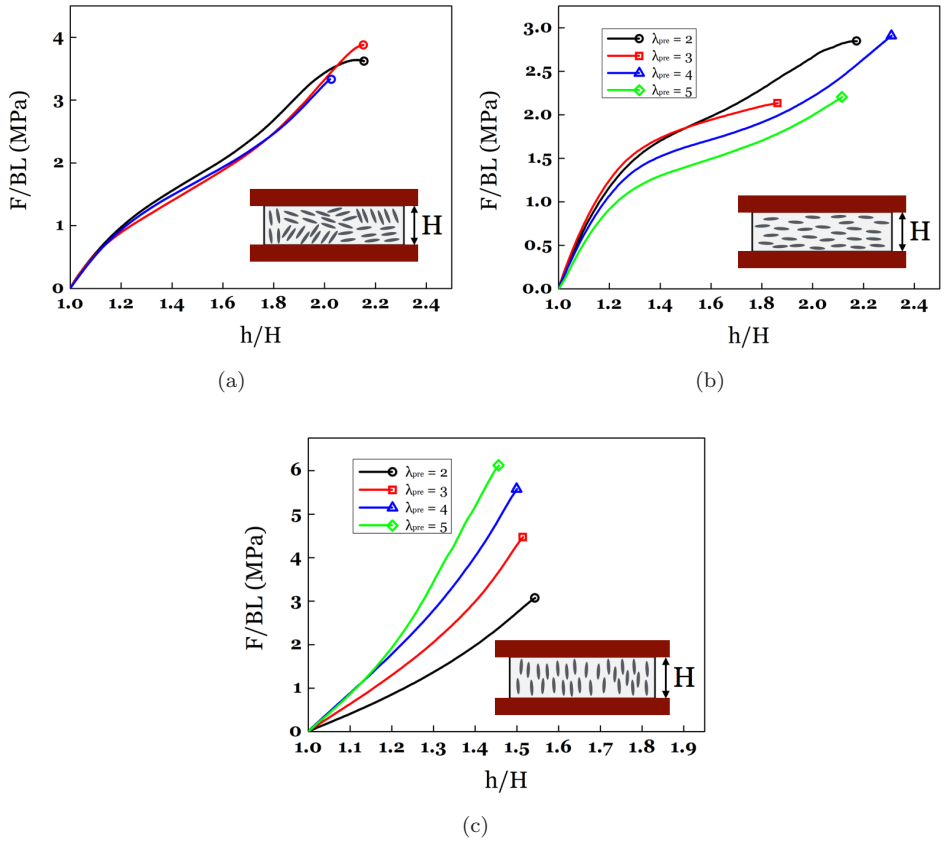

Fig. 3. Stress-stretch curves of pristine LCEs of different states under pure shear test. (a) Polydomain LCE; (b) Monodomain LCE with the loading direction perpendicular to the prestretch direction; (c) Monodomain LCE with loading direction parallel with the prestretch direction. The marks at the end of each curve represent rupturing points. In (b) and (c), three tests were conducted on the LCE samples for each condition, while only one representative curve for each condition was selected for the plot.

3.2. *Rupture of polydomain and monodomain LCEs*

3.2.1. *Stretch at rupture of LCEs with a precut*

Figures 4(a)–4(c) plot the stress-stretch curves of polydomain and monodomain LCEs with precut. Comparing Figs. 3 and 4, we find that the stretchability of LCEs is significantly reduced through the introduction of a precut with millimeter size. The effect of applied prestretch during LCE synthesis on stretch at rupture of precut LCEs is plotted in Fig. 5. Polydomain LCE samples have the largest stretch at rupture which is around 1.51 ± 0.03. The stretch at rupture decreases in the prestretched LCE samples when the loading direction is either perpendicular or parallel to the prestretch direction. It should be directly correlated with the fact that polydomain LCE has the largest fracture energy as discussed later. When prestretch

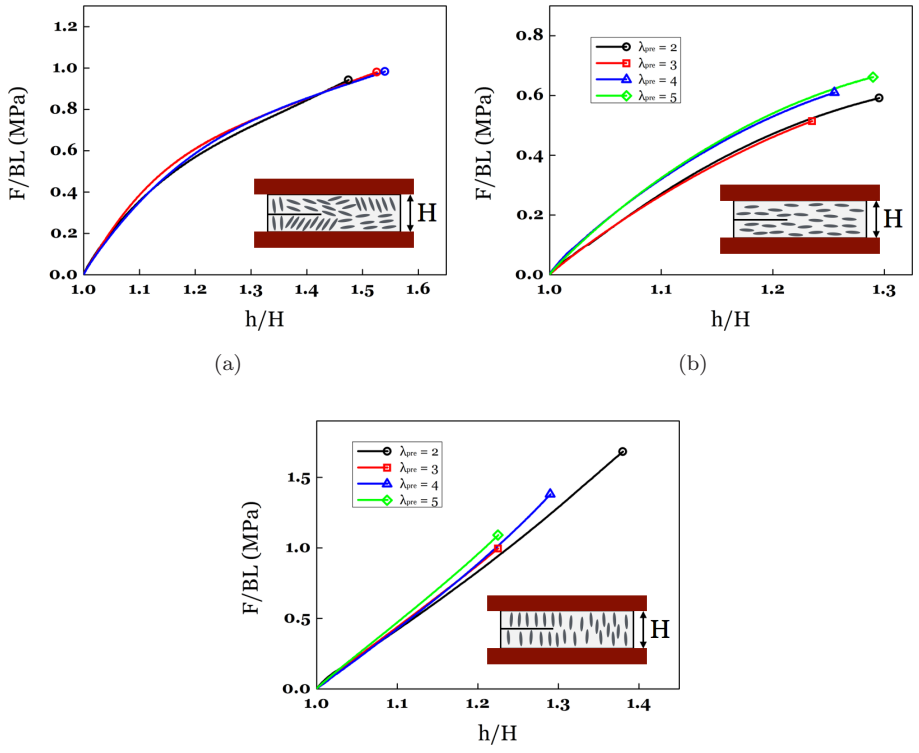

Fig. 4. Stress-stretch curves of LCEs of different states with a precut under pure shear test. (a) Polydomain LCE; (b) Monodomain LCE with the loading direction perpendicular to the prestretch direction; (c) Monodomain LCE with loading direction parallel with the prestretch direction. The marks at the end of each curve represent rupturing points. In (b) and (c), three tests were conducted on the LCE samples for each condition, while only one representative curve for each condition was selected for the plot.

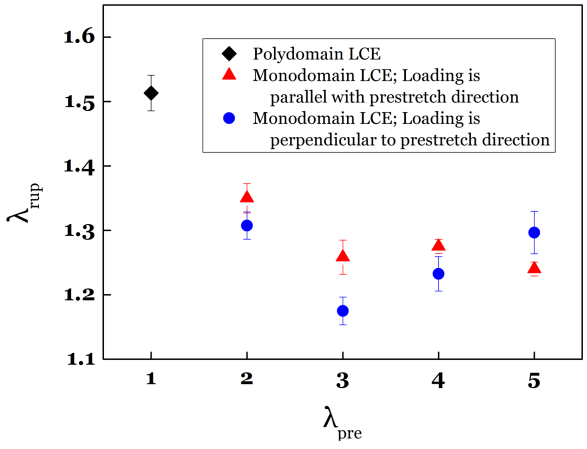

Fig. 5. The effect of applied prestretch during LCE synthesis on its stretch at rupture.

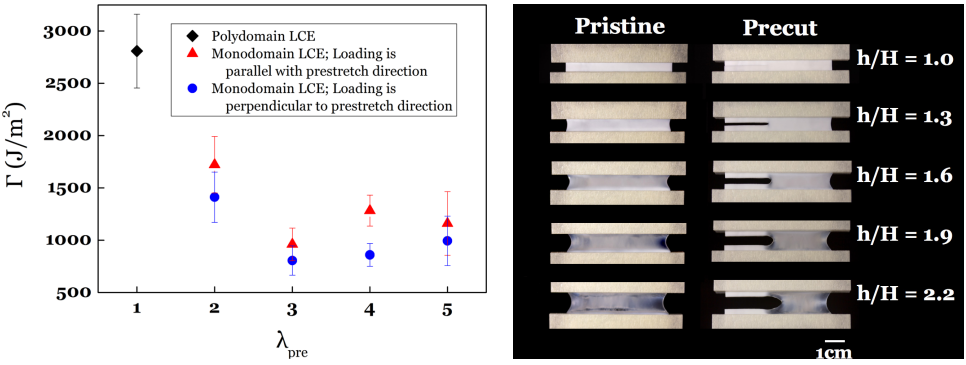

(a) (b)

Fig. 6. (a) Dependence of fracture energy of LCE on the applied prestretch during its synthesis. Fracture energy of polydomain LCE is almost two times of that of monodomain LCEs. (b) Photos of a pristine polydomain LCE sample and a precut polydomain LCE sample under pure shear test. When the stretch is larger than 1.6, the material near the crack tip changes from opaque to transparent, which is due to polydomain-to-monodomain transition induced by stretch. Such transition can dissipate additional energy, and thus increase fracture energy of polydomain LCE.

is beyond 3, the stretch at rupture for monodomain LCE samples is between 1.2 and 1.3 for both loading directions.

3.2.2. *Fracture energy of LCEs*

Figure 6(a) plots fracture energy of LCEs with different applied prestretches during their second crosslinking stage in the fabrication. It is clear that polydomain LCE, which corresponds to no applied prestretch during the synthesis, has the highest fracture energy ($2808 \pm 353\,\mathrm{J/m^2}$). When the LCE samples are prestretched beyond 3 during the preparation, the fracture energies of LCEs are reduced to the level around $1000\,\mathrm{J/m^2}$ for the loading directions both parallel with and perpendicular to the prestretch direction. It should be noted that we have verified that the measured fracture energies for different LCE samples do not depend on the dimensions of the sample and the precut. We believe that the significant increase of fracture energy in polydomain LCEs is mainly attributed to the stretch induced polydomain-to-monodomain transition near the crack tip of polydomain LCEs. As shown in Fig. 6(b), an initially opaque polydomain precut LCE sample becomes transparent near the crack tip when the stretch is large. As pointed out before [Clarke *et al.*, 1997], such optical transparency transition is due to the polydomain-to-monodomain transition induced by mechanical stretch. The toughening mechanism in polydomain LCE can be understood by examining the history of stress and strain of a material particle near the plane of the crack: when stretch is applied to the polydomain LCE sample with a precut, the material particle is gradually stretched and transit from polydomain to monodomain. After the crack front passes by the

material point, it is unloaded. The material particle undergoes large hysteresis due to the polydomain-to-monodomain transition, which dissipates extra energy and thus increase fracture toughness of polydomain LCE.

The fracture energy measured in the LCEs with loading direction parallel to the prestretch direction is consistently higher than that measured in the LCEs with loading direction perpendicular to the prestretch direction. Such direction-dependent fracture energy of LCEs is consistent with its anisotropic molecular structures.

3.2.3. *Predictions of rupture of polydomain LCEs under uniaxial tension*

As discussed by Rivlin and Thomas [1953], fracture energy of an elastomer should be independent of material geometry. Consequently, we can use the fracture energy of LCEs measured above to predict rupture of LCEs with different shapes and under different loading conditions. As an example, based on the previous measurements, we predicted the stretch at rupture of long strip polydomain LCEs with an edge crack of different sizes and subjected to a uniaxial tension.

For a long strip LCE as shown in the inset of Fig. 7(a), L, H, and B are used to denote its length, height, and thickness in undeformed state, and h is the height of the sample in the stretched state. In a precut sample, a small crack with initial length C is introduced in the middle by a razor blade, as shown in the inset of Fig. 7(b). In our experiments, L is 10 mm and H is 20 mm. Stretch rate is fixed as 0.3/min.

Figure 7(a) plots the measured stress-stretch curves of pristine polydomain LCE under uniaxial tension. Figure 7(b) plots stress-stretch curves of precut polydomain LCE with different crack sizes under uniaxial tension. Consequently, the dependence of stretch at rupture of LCE on the crack size can be obtained experimentally from Fig. 7(b).

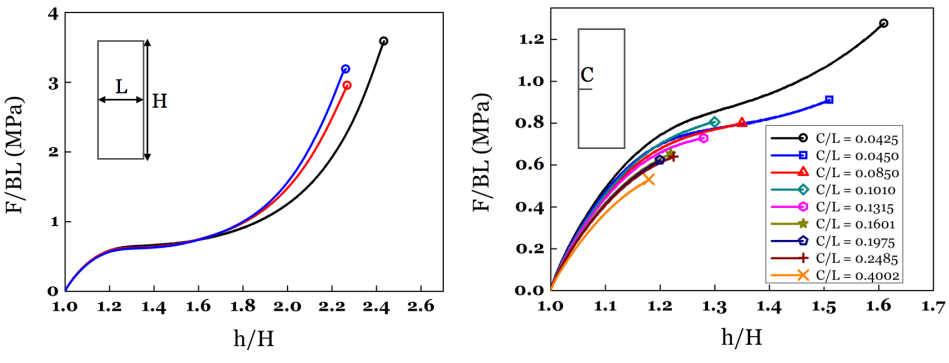

(a) (b)

Fig. 7. Stress-stretch curves of polydomain LCEs under uniaxial tensile tests. (a) Pristine sample; (b) Precut samples with different crack lengths. The marks at the end of each curve represent rupturing points.

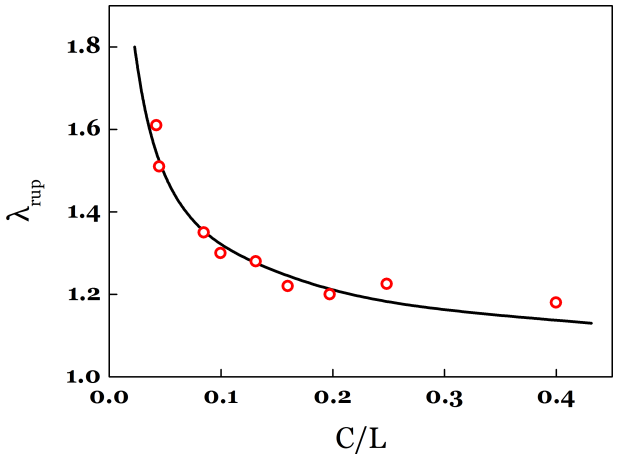

Fig. 8. Stretch at rupture of polydomain LCEs with a precut and under uniaxial tension. With the increase of crack length, C, the stretch at rupture decreases. The circles in the figure are experimental data and the solid curve is prediction.

Based on scaling analysis, energy release rate of a long strip elastomer under uniaxial tension can be given by,

$$G(\lambda) = 2k(\lambda) \cdot W(\lambda) \cdot C, \tag{2}$$

where k is a dimensionless function and W is strain energy density of the elastomer with uniaxial stretch. Following Lindley [1972], k is computed by the following equation: $k = \frac{2.95-0.08(\lambda-1)}{\sqrt{\lambda}}$, and W can be measured through uniaxial tension test of pristine sample.

By equating energy release rate computed from Eq. (2) to the fracture energy of polydomain LCE measured previously, we can predict the stretch at rupture of long strip polydomain LCEs containing an edge crack with different initial lengths under uniaxial tension. The prediction of the stretch at rupture of polydomain LCEs as a function of crack length is plotted together with experimental measurements in Fig. 8. We found that the predictions agree well with experimental measurement. The discrepancy between experiments and predictions increases when the crack length is large, which is mainly due to the inaccurate estimation of energy release rate from Eq. (2).

4. Conclusion

In this paper, we studied rupture in polydomain and monodomain LCEs. Using pure shear test, we measured fracture energy of LCEs with different applied pre-stretches during their synthesis. We found out that fracture energy in polydomain LCE is much higher than monodomain LCE, which may be attributed to stretch induced polydomain-to-monodomain transition in polydomain sample near its crack tip.

Acknowledgments

The work is supported by the National Science Foundation through Grant No. CMMI-1554212.

References

Adams, J. M. and Warner, M. [2005] "Soft elasticity in smectic elastomers," *Physical Review E* **72**(1), 011703.

Azoug, A., Vasconcellos, V., Dooling, J., Saed, M., Yakacki, C. M. and Nguyen, T. D. [2016] "Viscoelasticity of the polydomain-monodomain transition in main-chain liquid crystal elastomers," *Polymer* **98**, 165–171.

Biggins, J., Warner, M. and Bhattacharya, K. [2012] "Elasticity of polydomain liquid crystal elastomers," *Journal of the Mechanics and Physics of Solids* **60**(4), 573–590.

Brown, A. and Adams, J. [2012] "Negative Poisson's ratio and semisoft elasticity of smectic-C liquid-crystal elastomers," *Physical Review E* **85**(1), 011703.

Camacho-Lopez, M., Finkelmann, H., Palffy-Muhoray, P. and Shelley, M. [2004] "Fast liquid-crystal elastomer swims into the dark," *Nature Materials* **3**(5), 307–310.

Clarke, S. M., Nishikawa, E., Finkelmann, H. and Terentjev, E. M. [1997] "Light-scattering study of random disorder in liquid crystalline elastomers," *Macromolecular Chemistry and Physics* **198**(11), 3485–3498.

Corbett, D. and Warner, M. [2009] "Changing liquid crystal elastomer ordering with light — A route to opto-mechanically responsive materials," *Liquid Crystals* **36**(10–11), 1263–1280.

Dalhaimer, P., Discher, D. E. and Lubensky, T. C. [2007] "Crosslinked actin networks show liquid crystal elastomer behaviour, including soft-mode elasticity," *Nature Physics* **3**(5), 354–360.

Dawson, N. J., Kuzyk, M. G., Neal, J., Luchette, P. and Palffy-Muhoray, P. [2011] "Modeling the mechanisms of the photomechanical response of a nematic liquid crystal elastomer," *Journal of the Optical Society of America B* **28**(9), 2134–2141.

Dawson, N. J., Kuzyk, M. G., Neal, J., Luchette, P. and Palffy-Muhoray, P. [2011] "Cascading of liquid crystal elastomer photomechanical optical devices," *Optics Communications* **284**(4), 991–993.

Dey, S., Agra-Kooijman, D. M., Ren, W., McMullan, P. J., Griffin, A. C. and Kumar, S. [2013] "Soft elasticity in main chain liquid crystal elastomers," *Crystals* **3**(2), 363–390.

Finkelmann, H. and Shahinpoor, M. [2002] "Electrically controllable liquid crystal elastomer-graphite composite artifical muscles," *Proceedings of the SPIE's 9th Annual International Symposium on Smart Structures and Materials*, Vol. 4695, San Diego, United States of America, pp. 459–464.

Knight, D. P. and Vollrath, F. [2002] "Biological liquid crystal elastomers," *Philosophical Transactions of the Royal Society of London B*: *Biological Sciences* **357**(1418), 155–163.

Küpfer, J. and Finkelmann, H. [1991] "Nematic liquid single crystal elastomers," *Die Makromolekulare Chemie*, *Rapid Communications* **12**(12), 717–726.

Lehmann, W., Skupin, H., Tolksdorf, C., Gebhard, E., Zentel, R., Krüger, P., Lösche, M. and Kremer, F. [2001] "Giant lateral electrostriction in ferroelectric liquid-crystalline elastomers," *Nature* **410**(6827), 447–450.

Li, M.-H. and Keller, P. [2006] "Artificial muscles based on liquid crystal elastomers," *Philosophical Transactions of the Royal Society of London A*: *Mathematical*, *Physical and Engineering Sciences* **364**(1847), 2763–2777.

Lindley, P. [1972] "Energy for crack growth in model rubber components," *The Journal of Strain Analysis for Engineering Design* **7**(2), 132–140.

Petsch, S., Rix, R., Reith, P., Khatri, B., Schuhladen, S., Ruh, D., Zentel, R. and Zappe, H. [2014] "A thermotropic liquid crystal elastomer micro-actuator with integrated deformable micro-heater," *Proceedings of the 2014 IEEE 27th International Conference on Micro Electro Mechanical Systems* (*MEMS*), San Francisco, United States of America, pp. 905–908.

Rivlin, R. and Thomas, A. G. [1953] "Rupture of rubber. I. Characteristic energy for tearing," *Journal of Polymer Science* **10**(3), 291–318.

Schmidtke, J., Kniesel, S. and Finkelmann, H. [2005] "Probing the photonic properties of a cholesteric elastomer under biaxial stress," *Macromolecules* **38**(4), 1357–1363.

Schmidtke, J., Stille, W., Finkelmann, H. and Kim, S. T. [2002] "Laser emission in a dye doped cholesteric polymer network," *Advanced Materials* **14**(10), 746.

Shilov, S. V., Skupin, H., Kremer, F., Skarp, K., Stein, P. and Finkelmann, H. [1998] "Segmental motion of ferroelectric liquid crystal polymer and elastomer during electro-optical switching," *Proceedings of the Liquid Crystals*, *International Society for Optics and Photonics*, Vol. 3318, Zakopane, Poland, pp. 62–67.

Stenull, O. and Lubensky, T. C. [2005] "Phase transitions and soft elasticity of smectic elastomers," *Physical Review Letters* **94**(1), 018304.

Thomsen, D. L., Keller, P., Naciri, J., Pink, R., Jeon, H., Shenoy, D. and Ratna, B. R. [2001] "Liquid crystal elastomers with mechanical properties of a muscle," *Macromolecules* **34**(17), 5868–5875.

Warner, M. [1999] "New elastic behaviour arising from the unusual constitutive relation of nematic solids," *Journal of the Mechanics and Physics of Solids* **47**(6), 1355–1377.

Warner, M. and Terentjev, E. M. [2003] *Liquid Crystal Elastomers* (Oxford University Press, Oxford).

Xing, H., Li, J., Guo, J. and Wei, J. [2015] "Bio-inspired thermal-responsive inverse opal films with dual structural colors based on liquid crystal elastomer," *Journal of Materials Chemistry C* **3**(17), 4424–4430.

Yakacki, C., Saed, M., Nair, D., Gong, T., Reed, S. and Bowman, C. [2015] "Tailorable and programmable liquid-crystalline elastomers using a two-stage thiol — Acrylate reaction," *RSC Advances* **5**(25), 18997–19001.